Quenching of Chlorophyll Triplet States by Carotenoids in Reconstituted Lhca4 Subunit of Peripheral Light-Harvesting Complex of Photosystem I†

Donatella Carbonera,*,§ Giancarlo Agostini,|| Tomas Morosinotto,# and Roberto Bassi#

Dipartimento di Scienze Chimiche, Università di Padova, via Marzolo 1, 35131 Padova, Italy, CNR, Istituto di Chimica Biomolecolare, Sezione di Padova, via Marzolo 1, 35131 Padova, Italy, and Dipartimento Scientifico e Tecnologico, Università di Verona, Strada Le Grazie, 15-37234 Verona, Italy

Received February 11, 2005; Revised Manuscript Received April 15, 2005

ABSTRACT: In this study, triplet quenching, the major photoprotection mechanism in antenna proteins, has been studied in the light-harvesting complex of photosystem I (LHC-I). The ability of carotenoids bound to LHC-I subunit Lhca4, which is characterized by the presence of the red-most absorption components at wavelength >700 nm, to protect the system through quenching of the chlorophyll triplet states, has been probed, by analyzing the induction of carotenoid triplet formation. We have investigated this process at low temperature, when the funneling of the excitation toward the low-lying excited states of the Chls is stronger, by means of optically detected magnetic resonance (ODMR), which is well-suited for investigation of triplet states in photosynthetic systems. The high selectivity and sensitivity of the technique has made it possible to point out the presence of specific interactions between carotenoids forming the triplet states and specific chlorophylls characterized by red-shifted absorption, by detection of the microwave-induced Triplet minus Singlet (T-S) spectra. The effect of the red forms on the efficiency of triplet quenching was specifically probed by using the Asn47His mutant, in which the red forms have been selectively abolished (Morosinotto, T., Breton, J., Bassi, R., and Croce, R. (2003) *J. Biol. Chem. 278*, 49223−49229). Lack of the red forms yields into a reduced efficiency of the triplet quenching in LHC-I thus suggesting that the "red Chls" play a role in enhancing triplet quenching in LHC-I and, possibly, in the whole photosystem I.

Light harvesting is the first step in photosynthesis. The function is fulfilled in the thylakoid membranes of chloroplasts of higher plants by several pigment−protein complexes.

The outer antenna complexes of photosystem I, LHC-I[1], and photosystem II, LHC-II, all belong to Lhc multigenic family and have many common properties. Four Lhca proteins are associated with PSI (Lhca1−4) (*1*), while four more are found exclusively in PSII (Lhcb3−6). Lhcb1 and Lhcb2 are, together with Lhcb3, the building blocks of the major trimeric LHC-II complex which is generally found to be associated with PSII but can migrate to the unstacked stroma membranes and bind to PSI upon phosphorylation (*2*), thus allowing energy redistribution between the two photosystems in conditions of unbalanced excitation (*3*). Lhc proteins bind several Chl *a*, Chl *b*, and xanthophyll chromophores, and the pigment composition and the spectral properties are tuned specifically in each Lhc gene product (*4*).

The recent crystal structure of spinach LHC-II complex at 2.72 Å resolution (*5*) has revealed the organization of the pigments and their coordination to the protein residues in more detail compared to previous models (*6*), including the location of the 14 chlorophylls, eight Chl *a*, and six Chl *b* within one monomeric LHC-II complex. Three carotenoid molecules were also identified as two luteins and one neoxanthin, located, respectively, in sites L1, L2, and N1. The fourth xanthophyll molecule, located in binding site V1 (*7*), was found at the interface between interacting monomers and showed mixed occupancy by violaxanthin and zeaxanthin. The X-ray crystal structure of PSI from pea at 4.4 Å resolution (*8*) shows that the reaction center and the four antenna proteins (Lhca1−4) constituting LHC-I, form two loosely associated units in which the Lhca1−4 polypeptides make a crescent folded around one side of the reaction center complex. The organization of Lhca subunits into dimers is unique of PSI antenna system and is likely to be instrumental to efficient energy transfer to the core pigments. As expected from the high sequence homology, the helix structure and the general fold of LHC-I and LHC-II polypeptides are quite similar (*8*). Despite homology, however, LHC-I is characterized by peculiar low-energy absorption forms of chlorophyll, responsible for the 77 K fluorescence emission maximum at 730 nm (*9*). LHC-I has a high-pigment density which may be responsible for the observed red-shifted spectral characteristics; however, a number of experimental data obtained with recombinant Lhca1−4 apoproteins show that these proteins are able to produce red-shifted forms even as isolated monomers (*9*−*12*). In accordance with these results, the red-

† This work was supported by the Italian Ministry for University and Research (MURST) under the project FIRB RBAU01E3CX "Meccanismi molecolari della Fotosintesi".

* Corresponding author: phone, +39-049-827-5144; fax, +39-049-827-5161; e-mail, donatella.carbonera@unipd.it.

§ Università di Padova.

|| CNR, Istituto di Chimica Biomolecolare.

Università di Verona.

[1] Abbreviations: Car, carotenoid; Chl, chlorophyll; Lut, lutein; LHC-I, light-harvesting complex of photosystem I; LHC-II, light-harvesting complex of photosystem II; ODMR, optically detected magnetic resonance; FDMR, fluorescence-detected magnetic resonance; ADMR, absorbance-detected magnetic resonance; ZFS, zero field splitting; ISC, intersystem crossing; WT, wild-type; N47H mutant, Lhca4-Asn47His mutant.

10.1021/bi050260z CCC: $30.25
Published on Web 05/19/2005

most absorption is associated with Lhca4 (*9*), but red shifted absorption forms are found in all Lhca1−3 complexes although with different amplitudes and transition energies.

Since the carotenoid binding sites are not resolved in the electron density map of LHC-I reported up to now, similarities and differences among LHC-II and LHC-I polypeptides may only be inferred from biochemical experiments. In accordance with Croce et al. (*13*) and Castelletti et al. (*12*), two of the four Lhca proteins, that is, Lhca1 and Lhca3, bind three xanthophylls, while Lhca4 and -2 each binds only two xanthophyll molecules per polypeptide. In particular, the Lhca4 complex binds 0.5 violaxanthin and 1.5 lutein molecules in the two central sites, L1 and L2. By analogy with CP29 (Lhcb4), CP26 (Lhcb5), and CP24 (Lhcb6), which also bind two xanthophylls per polypeptide, it has been suggested that the xanthophyll binding sites conserved in Lhca4 correspond to L1 and L2 sites of LHC-II (*13*), a hypothesis later confirmed by mutational analyses of Lhca4 (Morosinotto et al., personal communications).

It is well-known that carotenoids play an important role in photoprotection of LHC-II through multiple mechanisms: lutein in site L1 is active in quenching triplet chlorophyll states (*14*) thus preventing the formation of singlet oxygen ($^1O_2$*), and subsequent harmful oxidation (*15*). Moreover, zeaxanthin binds to the allosteric site L2 thus inducing a conformational change in LHC-II (*14*) and fluorescence quenching. Zeaxanthin is produced in high-light conditions through the de-epoxidation of violaxanthin by VDE (violaxanthin de-epoxidase) activated by low lumenal pH (*16*). LHC-I proteins, in addition to these above-described mechanisms, exhibit a low-fluorescence yield due to the presence of an "intrinsic dissipative conformation" for Lhca polypeptides, as suggested in ref *17*.

The triplet quenching mechanism is likely to occur also in LHC-I complexes, given the presence of xanthophylls located close to Chl molecules, although only preliminary results for carotenoid triplet states associated to PSI have been obtained so far (*18*). It is possible that the carotenoids actively participate in tuning the spectral properties of the nearby Chl a molecules through direct electronic interaction, as suggested by the close proximity of Chl A3 and B6 to xanthophylls bound to sites L1 and L2, respectively. In fact, site-directed mutagenesis at each Chl binding residue yielded into loss of the nearby xanthophyll molecule (*17*).

In the past, the study of Car triplet states formed in LHC-II complexes has been performed by means of different techniques (EPR, ODMR, time-resolved optical spectroscopy (*19*−*23*)), leading to the characterization of different carotenoid triplet states, showing specific interactions with nearby Chl molecules (*19*−*23*). Recently, based on the crystallographic structure, the carotenoid triplet states observed under illumination of isolated trimers of LHC-II at low temperature have been assigned to carotenoids sitting in L1 and L2 sites (*23*). The assignment is, however, still controversial in view of the dependence of the results on the preparations and of the spectral superimposition of different carotenoids bound to the complex.

The present work addresses the question of the ability of the LHC-I complex to populate carotenoid triplet states. By analyzing the induction of triplet formation in the recombinant protein Lhca4, we have investigated the activity of the carotenoids in quenching triplet states at low temperature when the funneling of the excitation toward the low lying excited states of the Chl molecules is fast (*25*). We used optically detected magnetic resonance (ODMR) techniques which are well-suited for investigation of triplet states in photosynthetic systems (*26*−*29*). The selectivity and sensitivity of these techniques make it possible to point out the presence of specific interactions between carotenoids forming the triplet states and Chls, by detection of the microwave-induced Triplet minus Singlet (T-S) spectra.

It has recently been demonstrated that substitution of the Asn coordinating the Chl *a* molecule in the A5 binding site of Lhca4 by His, abolishes the red spectral forms of native Lhca4 without affecting the number of bound Chl molecules (*10*). Therefore, we have extended the ODMR analysis to the Lhca4-N47H mutant with the aim of verifying the relation between the presence of red-shifted spectral forms and the quenching of chlorophyll triplet states by carotenoids, the localization of the carotenoid-triplet states, and the interaction between carotenoid and chlorophyll pairs.

MATERIALS AND METHODS

Reconstitution and Purification of Pigment−*Protein Complexes.* Apoproteins of Lhca4 WT and N47H mutant from *Arabidopsis thaliana* were expressed and isolated from the SG13009 strain of *Escherichia coli* as described in ref *10*. Refolding and purification of Lhca4 were performed as described in ref *29*.

Pigment Analysis. HPLC analysis was as in ref *30*. Chlorophyll-to-carotenoid ratio and Chl *a*/Chl*b* ratio were independently measured by fitting the spectrum of acetone extracts with the spectra of individual purified pigments (*31*).

ODMR Experiments The samples were diluted to a final Chl concentration equivalent to 100 μg/mL, and 60% v/v glycerol was added to obtain a transparent glass upon cooling of the sample to the cryogenic temperature of the experiments. Fluorescence-detected magnetic resonance (FDMR) and absorption-detected magnetic resonance (ADMR) experiments were performed in the same home-built apparatus, previously described in detail (*25*−*26*). The flexibility of the set up allows us to perform both kind of experiments on the same sample by switching the detection mode. The ODMR is a double resonance technique based on the simple principle that, when upon illumination, a triplet steady-state population is generated in a system, the application of a resonant microwave electromagnetic field between a couple of spin sublevels of the triplet state generally induces a change of the steady-state population of the triplet state itself, due to the anisotropy of the decay and population rates of the three spin sublevels. The induced change of the triplet population may be detected as a corresponding change of the emission and/or absorption of the system (*32*). Amplitude modulation of the applied microwave field it used to greatly increase the signal-to-noise ratio by means of a phase sensitive lock-in amplifier (EG&G 5220). In the FDMR experiments, the fluorescence, excited by a halogen lamp (250 W) focused into the sample and filtered by a broadband 5 cm solution of 1 M $CuSO_4$, was collected at 45° through appropriate band-pass filters (10 nm fwhm) by a photodiode before entering the lock-in amplifier. Low-temperature emission spectra were detected in the same apparatus used for ODMR experiments, using the same excitation source, but substitut-

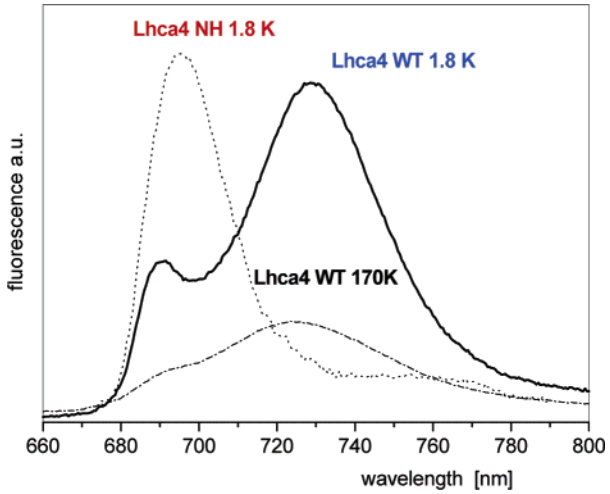

FIGURE 1: Fluorescence emission spectra of Lhca4 at 1.8 K (solid) and at 170 K (dashed−dot) and of Lhca4-N47H mutant at 1.8 K (dots).

ing the band-pass filters before the photodiode, coupled to a voltage-amplifier, by a monochromator. In the absorption detection mode (ADMR), the same excitation lamp was used but without filters before the sample, except for a 5 cm water and heat filters. The beam was focused into the monochromator after passing the sample and finally collected by a photodiode. The modulation frequency and the microwave power were chosen depending on the experiment. By fixing the microwave frequency at a resonant value while sweeping the detection wavelength, Triplet -minus-Singlet (T-S) spectra can be registered. The temperature was 1.8 K for most of the experiments. At such a temperature, spin−lattice relaxation is inhibited and the ODMR signal is maximum. In the experiments at higher temperatures, the helium flow in the cryostat was adjusted to obtain stable temperature ranging from 1.8 up to 240 K.

RESULTS

Lhca4-WT. The absorption spectrum of Lhca4 at room temperature was characterized by a red absorption tail at wavelengths longer than 700 nm, and the fluorescence emission showed a maximum at 686 nm and a shoulder at 720 nm, in agreement with previous results (*10*). At 1.8 K, the fluorescence maximum was further red-shifted to about 735 nm as shown in Figure 1.

Illumination of the sample at cryogenic temperatures induces the formation of triplet states which can be detected by monitoring the emission of the sample while sweeping the microwave field in the spectral region where chlorophyll and carotenoid triplet states are expected to show resonant spin transitions. In principle, FDMR should not be suitable for detection of carotenoid triplet states, since carotenoids are nonfluorescing molecules; however, it has been previously demonstrated (*25*, *27*) that, due to the energy transfer processes going on among carotenoids and chlorophylls in the antenna complexes, a change of the steady-state population of the carotenoid triplet states, induced by a resonant microwave field, is reflected by a change of the intensity of the emission of the nearby chlorophyll molecules. In Figure 2, the FDMR spectra detected at different wavelengths of the emission spectrum (690−740 nm) and in the microwave

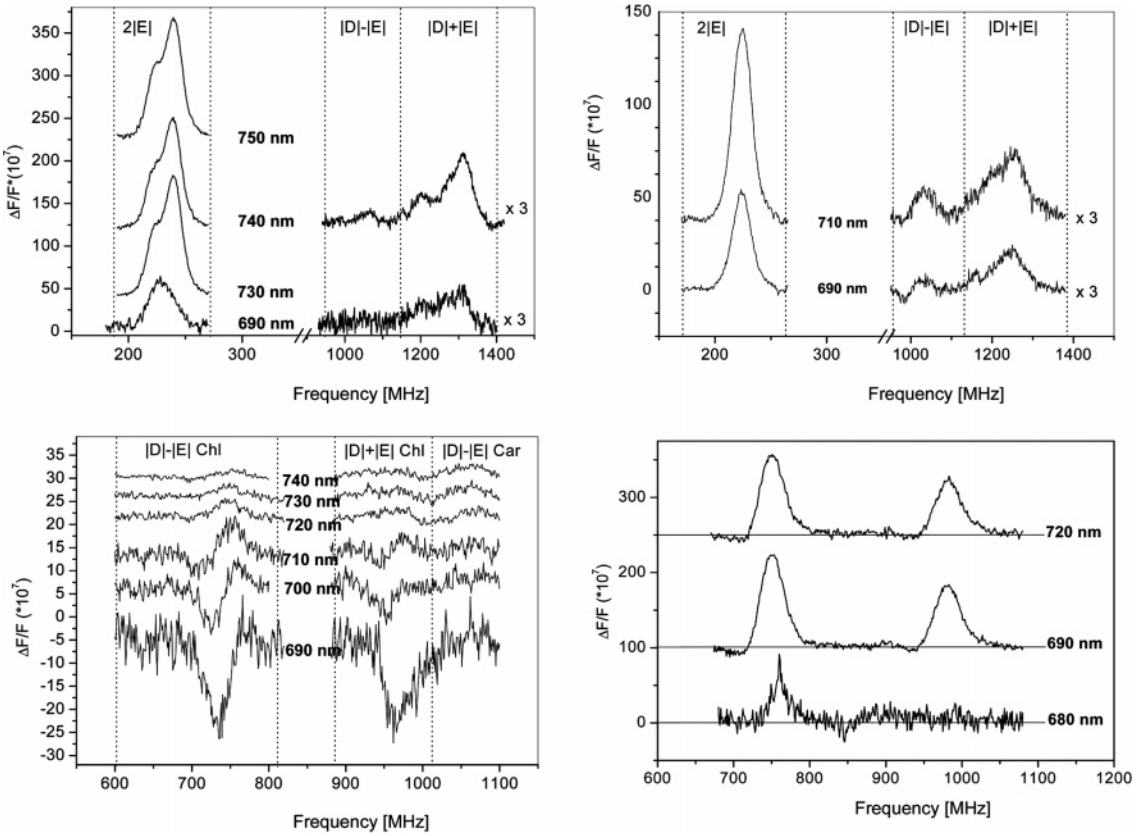

FIGURE 2: FDMR spectra of Lhca4 and Lhca4-N47H at 1.8 K detected at different wavelengths as indicated. Left panels, Lhca4; right panels, Lhca4-N47H. Top panels, FDMR of carotenoid triplet states; mod. freq 323 Hz, mw power 1 W. Bottom panels: FDMR of chlorophyll triplet states; mod. freq 33 Hz, mw power 0.5 W. The traces have been vertically shifted for a better comparison.

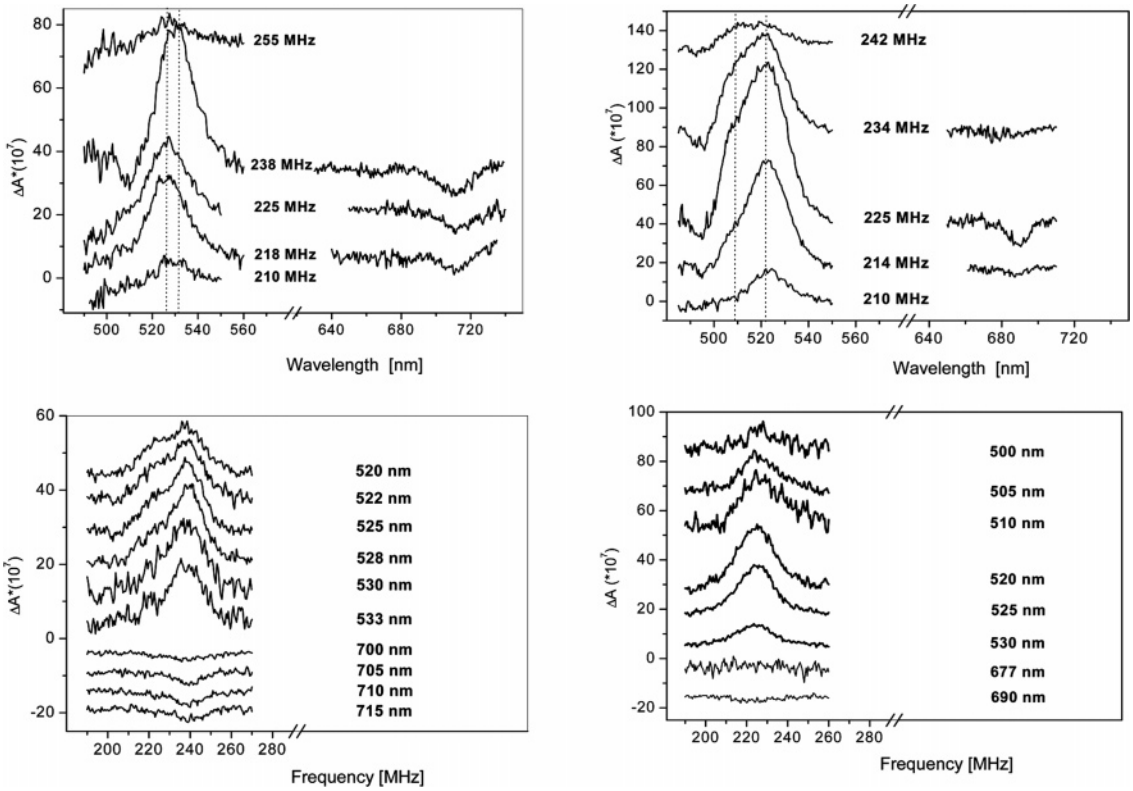

FIGURE 3: Top panels, T-S spectra of Lhca4 (left) and Lhca4-N47H (right) at 1.8 K detected at different resonant microwave frequencies in the 2|*E*| transition of carotenoids, as indicated. The traces have been vertically shifted for a better comparison. Mod. freq 323 Hz, mw power 1 W. Bottom panels, ADMR spectra of Lhca4 (left) and Lhca4-N47H (right) showing the contribution to the 2|*E*| transition when detecting the absorption change at different wavelengths as indicated. Mod. freq 323 Hz, mw power 1 W.

field region where the 2|*E*|, the |*D*| − |*E*|, and the |*D*| + |*E*| transitions of carotenoids are expected on the basis of the analogy with the LHC-II complex (*20*, *25*) are shown. Three transitions with the polarization pattern usually found for carotenoids (intensity of 2|*E*| ≫ |*D*| + |*E*| > |*D*| − |*E*|) have been detected, proving the ability of the Lhca4 complex to quench Chl triplet states by populating carotenoid triplets, even at very low temperature.

The spectra show, for each transition, a complex and wavelength-dependent line shape suggesting the presence of different components contributing to the whole triplet population. Hole-burning experiments, performed by using a microwave field at a fix resonant frequency while sweeping a second microwave field, show that the homogeneous broadening of the 2|*E*| transition, at 1.8 K, is about 5 MHz (not shown). In Figure 2, the spectral region where the |*D*| − |*E*| and the |*D*| + |*E*| transitions of Chl *a* triplet states have been found in several photosynthetic systems (*25*, *27*) is also shown. The signals are weak meaning that Chl triplet states are present only in small amounts; however, the presence of few different components is clearly seen. The 2|*E*| transitions, as usually found for Chl triplet states, were too weak to be detected. The |*D*| + |*E*| transition of Chl triplet state, at about 1000 MHz, partially overlaps the |*D*| − |*E*| transition of the carotenoids. Nevertheless, because of the different lifetimes of the two kind of triplets, microseconds for carotenoid versus milliseconds for Chl triplet states, it is possible to discriminate between them by choosing the suitable modulation frequency of the microwave field. In particular, the contribution of Chl triplet states to the spectra recorded at 323 Hz, the modulation frequency which optimizes the carotenoid contribution, is negligible (Figure 2, left upper panel).

To characterize the triplet states in terms of the absorption spectra of the different species contributing to the FDMR transitions, the microwave-induced T-S spectra were taken at different frequencies and the ADMR spectra were also detected at different significant wavelengths. The results are shown in Figure 3 for the carotenoids and in Figure 4 for the chlorophylls.

From the T-S spectra taken at different frequencies set in the most intense transition of carotenoids, that is, the 2|*E*| transition, it can be derived that the T-T absorption band, which is the main feature in the T-S spectrum of carotenoids and which always appears to the red side of the red-most $S_0 \rightarrow S_2$ absorption band, is centered at 525 nm for the carotenoid population(s) showing a lower microwave frequency resonant transition (at about 220 MHz), while it is centered at about 530 nm for the transition at 240 MHz, corresponding to the main peak in the FDMR spectra. The T-T absorption bands are partially superimposed by the corresponding bleaching bands of the carotenoid singlet−singlet absorption ($S_0 \rightarrow S_2$). In the Chl Q_y absorption region, an additional weak band is also detected. This band can be assigned to an "interaction band" between Chl and Car molecules, based on analogous results obtained in several light-harvesting complexes belonging to both bacteria and plants (*20*, *33*). Interestingly, the band corresponds to the bleaching of the red-most (710 nm) absorbing Chl *a* molecules and is very broad, as already observed for the tail of the absorption spectrum extending to long wavelengths (*10*). It seems that all the carotenoid triplet populations,

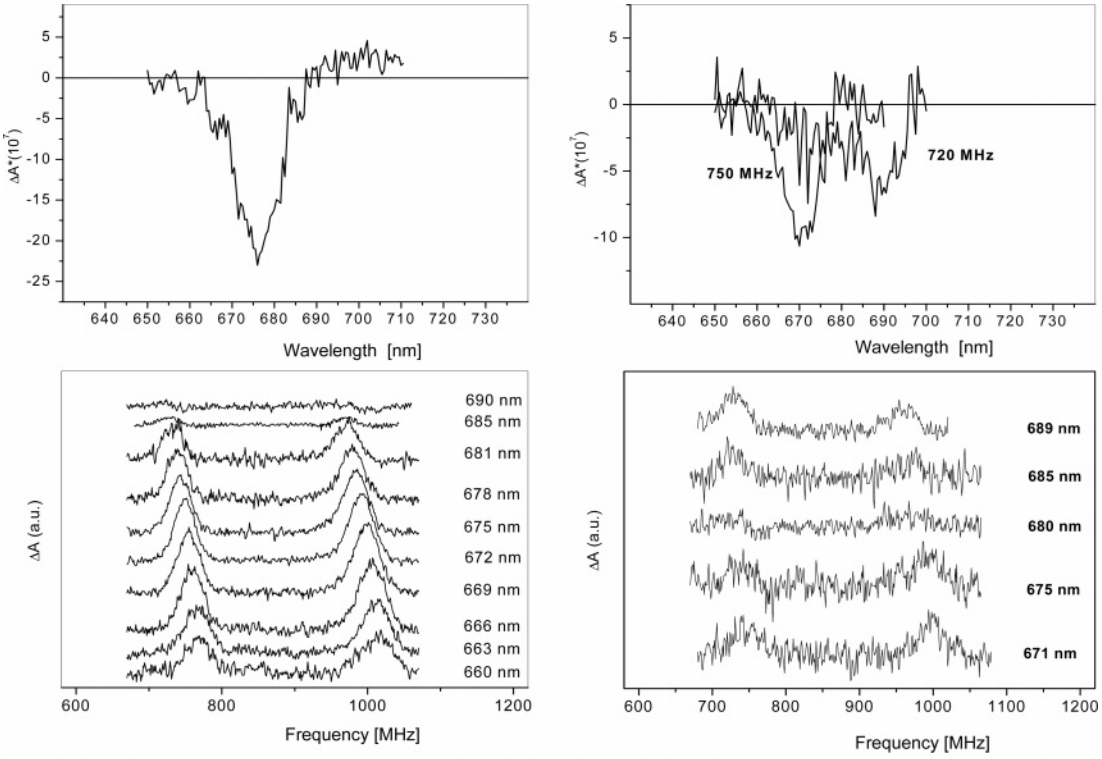

FIGURE 4: Top panels, T-S spectra at 1.8 K of Lhca4 (left), detected at the resonant 732 MHz ($|D| - |E|$ transition of Chl triplet) and of Lhca4-N47H (right) detected at the two main resonant frequencies 750 and 720 MHz ($|D| - |E|$ transition of Chl triplet). Mod. freq 33 Hz, mw power 0.5 W. Bottom panels, ADMR spectra of Lhca4 (left) and Lhca4-N47H (right) at 1.8 K showing the $|D| - |E|$ and the $|D| + |E|$ transitions of Chl triplets when detecting the absorption change at different wavelengths as indicated (bands are shown as positive even though they represent bleachings). Mod. freq 33 Hz, mw power 0.5 W.

selected by different microwave frequencies, interact with the red-absorbing chlorophylls. There is no evidence of Car−Chl *b* interaction bands in the T-S spectra.

Together with the carotenoid triplet states, also chlorophyll triplet states are present in our experimental conditions, meaning that the efficiency of the T-T transfer to carotenoids, at the low temperature of the experiments, is not complete. The FDMR results (Figure 2 left, bottom panel) show that Chl triplet states may be detected across the whole emission spectrum even though the signals are very weak, especially at longer wavelengths. Because of the energy transfer processes among Chls which take place in the complex, the assignment of these triplet states to a particular Chl pool may not be inferred directly from the FDMR experiments since it is in principle possible to observe a FDMR signal of a nonfluorescing molecule if this is connected via energy transfer to an emitting one (*35*). In the T-S spectrum associated to the maximum of the resonance, 732 MHz, reported in Figure 4, the absorption of the Chl *a* molecules giving the triplet states is seen as a bleaching peaking at 675 nm. In the ADMR spectra, shown in Figure 4, taken at different wavelengths in the Chl *a* Q_y absorption band, it is possible to assign a precise absorption to all the components detected in the FDMR spectra. The absorption of such components is more or less spread in the spectral region between 660 and 685 nm. However, no long-absorbing wavelength components have been detected meaning that the quenching of triplet states of red-absorbing Chls operated by the carotenoids present in the complex is very efficient.

The intensity of the ODMR signals of carotenoid and chlorophyll triplet states undergoes a temperature -induced decrease due to the increase of the rate of the thermal spin−lattice relaxation. In fact, in the first temperature range (1.8−70 K), the signal intensity decays rapidly (Figure 5); this effect is usually observed in ODMR experiments in zero field for triplet states of organic molecules and is due to activation of a fast spin−lattice relaxation which is responsible for termalization of the populations of the three spin sublevels. Surprisingly, further increase of the temperature, ranging between 70 and 160 K leads to an increase of signal intensity with a polarization pattern which is quite different with respect to the low-temperatures one: the $2|E|$ transition becomes almost as intense as the $|D| - |E|$ transition, while the $|D| + |E|$ transition becomes undetectable. In this temperature range, the spin−lattice relaxation seems to become slow again compared to other dynamic processes allowing a steady-state polarization of the populations. Although a similar behavior has been previously reported for carotenoid triplet states of photosynthetic antenna systems of bacteria and algae (*35*, *36*), the origin of the phenomenon remains obscure. The transitions are still inhomogeneously broadened; however, the number of components which are required to fit the experimental data is reduced with respect to 1.8 K (see Discussion). Above 160 K, the signal starts to decrease again under the effect of the further increased relaxation. Moreover, the ZFS parameters continuously change showing a decrease, especially of the $|E|$ value with the temperature, indicating either a more symmetric electronic distribution in the molecules or a change of the molecular environment (Figure 5).

The same temperature dependence of the FDMR signals is also present in the ADMR experiments (Figure 5), even though the spectra are more noisy because of the weakness of the signals, showing that the effects are not limited to a

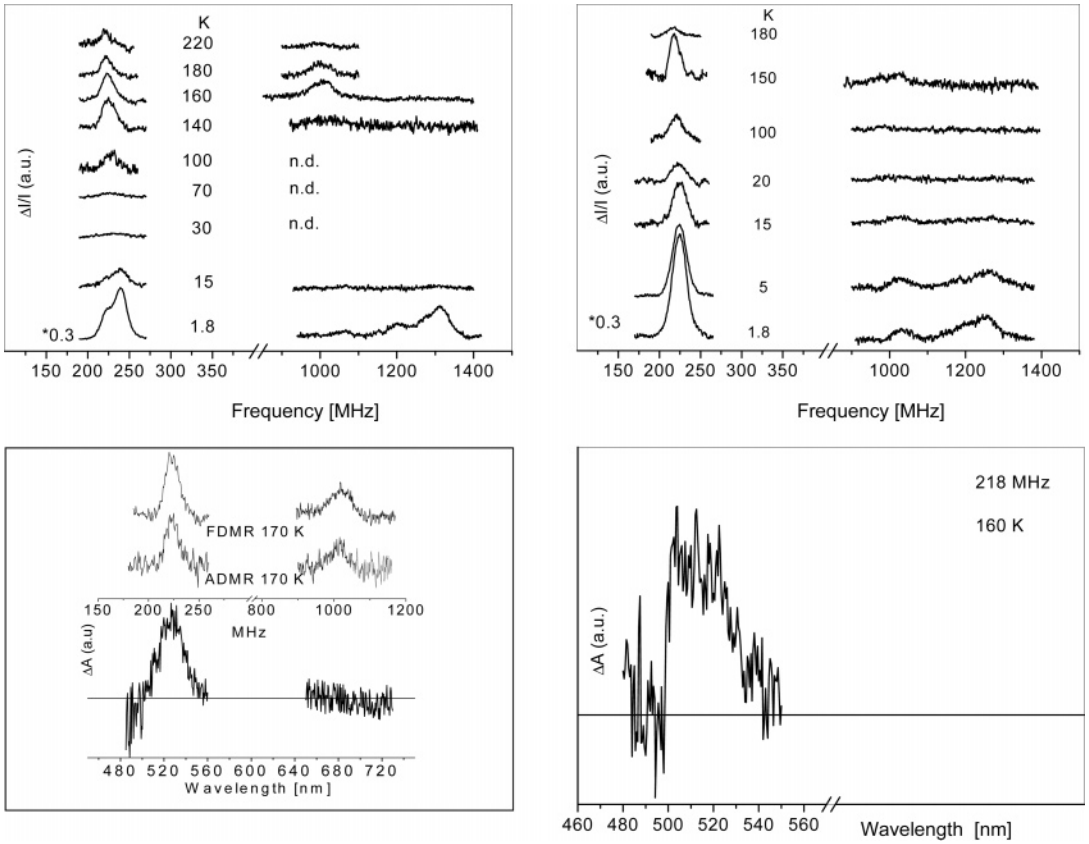

FIGURE 5: Top panels, FDMR spectra of Lhca4 (left) and Lhca4-N47H (right) detected at 740 nm at different temperatures as indicated. Mod freq 323 Hz, mw power 2 W. Bottom left panel, upper part, comparison of the FDMR and ADMR spectra of Lhca4 at 170 K; lower part, T-S spectrum of Lhca4 detected at 170 K and at the maximum of the 2|*E*| transition. Bottom right panel, T-S spectrum of Lhca4-N47H detected at 170 K and at the maximum of the 2|*E*| transition.

particular triplet population selected by the emission detection at 740 nm, but involve the bulk carotenoid triplet state population. The T-S spectrum detected at the maximum of the 2|*E*| transition at 170 K (Figure 5), shows a broad T-T absorption peaking at 527 nm. Unfortunately, the signal is too weak to observe a significant change of the absorption in the Q_y absorption region of chlorophyll molecules.

Lhca4-N47H mutant. The absorption spectrum of the Lhca4-N47H mutant used for the present experiments is lacking the red absorption tail at wavelengths longer than 700 nm, as already reported (*10*). Correspondingly, the fluorescence emission is blue-shifted as compared to the WT, and at 1.8 K, the maximum is found at about 695 nm (see Figure 1). The same kind of experiments reported above for the Lhca4 have been performed also on the N47H-mutant. The results are reported in Figures 2−4, right panels, for a direct comparison with the results concerning the WT and described above. Again, carotenoid triplet states have been detected by monitoring the change of the fluorescence intensity of chlorophylls.

The line shape of the three FDMR transitions is not wavelength-dependent, although a few components give contribution to each transition as in the case of the WT (see Discussion). Chl triplet states are also populated by illumination at low temperature, and the their FDMR are more intense, relative to the carotenoid contributions, with respect to those detected in Lhca4 (Figure 2).

In the T-S spectra of the mutant, detected at different mw frequencies selected in the most intense 2|*E*| transition of carotenoids, Figure 3, the strong T-T absorption bands exhibit two distinct peaks at about 505 and 525 nm. The different contributions to these T-T absorption bands, in terms of 2|*E*| transition, are also shown in Figure 3, where the ADMR spectra recorded at different wavelengths are reported. The T-S spectrum shows also, in the Q_y absorption region of Chls, the bleaching assigned to the Car−Chl interaction band. At all the frequencies, the negative band is blue-shifted (<700 nm) with respect to the WT. The ADMR spectra detected at various wavelengths show the different contribution of the 2|*E*| transition to the T-S spectra.

The chlorophyll giving the triplet states upon illumination at low temperature may be divided into two main populations based on the T-S and ADMR spectra reported in Figure 4, having the Q_y absorption band centered respectively at 675 and 689 nm. The ODMR signals of carotenoid triplet states undergo the same temperature-induced behavior as already observed for the WT, in terms of both the relative intensity and the polarization pattern of the signals (Figure 5). Also in this case, the $|D| + |E|$ transition is not detectable at high temperatures. The results are confirmed by the ADMR experiments (not shown).

In Figure 5, the T-S spectrum at 160 K, taken at 218 MHz, the maximum of the 2|*E*| transition at this temperature, is reported. It shows a broad T-T absorption covering the whole band detected at 1.8 K.

DISCUSSION

Lhca4-WT. The presence of long absorbing Chl *a* molecules in PSI is associated with the peripheral light-harvesting

complex LHC-I, which, for this reason, becomes a site of probable Chl triplet formation and then of photodamage for the system. However, in the present study, we show that the xanthophylls belonging to Lhca4, which is responsible for the reddest emission of the of LHC-I complex, are able to operate the chlorophyll triplet quenching. Even at the very low temperature of ODMR experiments, 1.8 K, at which the excitation is largely sitting in the red forms of chlorophylls (*24*), no chlorophyll triplet states of the red-absorbing molecules have been detected, suggesting that carotenoids are very efficient in the quenching of the triplet states which are likely populated via ISC in the red forms.

The FDMR spectra of carotenoids, obtained at various detection wavelengths, have been fitted by a global Gaussian analysis deconvolution since their complex line shape indicates the presence of different components. It must be noted that a simultaneous fitting over the three transitions ($2|E|$, $|D| + |E|$, $|D| - |E|$) belonging to the same triplet has the constrain of the relationship occurring between the ZFS parameters and the energy of the transitions, meaning that, to obtain a global satisfying deconvolution for each triplet, the position of the peak frequencies of the $2|E|$, $|D| - |E|$ and $|D| + |E|$ transitions must be obtained with the same $|D|$ and $|E|$ values. The minimum number of components which gives the best global fit is four. Further increase of the number of the components does not improve the fitting significantly. The same components are found in the spectra at all the wavelengths detected but with different amplitudes (see Supporting Information). The four triplet components have similar line widths and polarization patterns ($2|E| \gg |D| + |E| > |D| - |E|$), as reported in Figure 6 where the fittings of FDMR spectra, detected at two different wavelengths, are shown as examples. The order of the assignment has been tested in some cases by double resonance experiments (not shown). Several set of independent experiments have been simulated giving the averaged ZFS parameters reported in Table 1. The same components obtained from the fitting of the FDMR spectra have also been used for the analysis of the $2|E|$ transitions in the ADMR spectra, the only one having a sufficient amplitude to be analyzed. Good fits are obtained by changing only the amplitude of the contributing triplets but not the resonant frequencies determined by FDMR. The T-T absorption bands, corresponding to the different components in the frequency domain, which have been reconstructed on the basis of the contribution of different components in the ADMR spectra, are shown in Figure 6 (see Supporting Information for details). They differ from each other only by few nanometers, the main component having the maximum of the T-T absorption centered at 528 nm. Other two components have about 1/3 amplitude and are centered at 525 nm. A forth minor component is centered at about 530 nm.

The stoichiometry of the carotenoid content of the Lhca4 recombinant sample, reported in Table 2, does not seem to be related to the relative amplitudes of the four triplet components observed in the spectra in a simple way. Carotenoids may function in photoprotection by quenching $^1O_2$* or by preventing its formation from ^{3}Chl*. Protection from photobleaching shows that xanthophylls in both the L1 and L2 sites of trimers of LHC-II are active in photoprotection even at cryogenic temperatures (*23*), while only the L1 site is active in monomers. In LHC-II complex, relatively

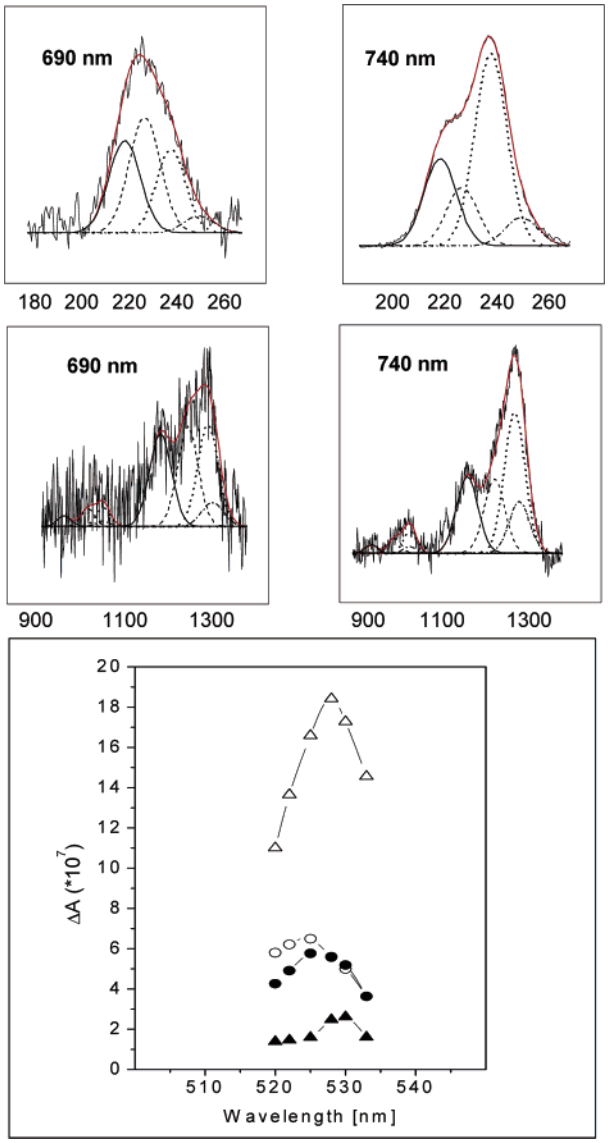

FIGURE 6: Top panel, fitting of FDMR spectra at 690 and 740 nm, normalized to their maximum to better show the Gaussian components contribution to the reconstruction. Bottom panel, T-T absorption bands relative to each of the four components, reconstructed on the basis of the fitting of the $2|E|$ ADMR transitions, reported in Table 1 (open circles, T_1; filled circles, T_2; open triangles, T_3; filled triangles, T_4).

Table 1: ZFS Parameters of the Four Components of the Global Fit of FDMR and ADMR Spectra of Carotenoids

components (1.8 K)	$\|D\|$ (cm^{-1})	$\|E\|$ (cm^{-1})
T_1	364.3×10^{-4}	36.7×10^{-4}
T_2	383.6×10^{-4}	38.2×10^{-4}
T_3	397.2×10^{-4}	40.0×10^{-4}
T_4	398.9×10^{-4}	42.0×10^{-4}
components (160 K)	$\|D\|$ (cm^{-1})	$\|E\|$ (cm^{-1})
T_1	364.1×10^{-4}	33.5×10^{-4}
T_2	378.5×10^{-4}	37.8×10^{-4}

red Chls are thought to be located close to the L1 site and carotenoids in L1 site contribute mostly to populate triplet states (37).

In view of the fast energy transfer to the red forms occurring in the Lhca4 complex (*24*), it is unlikely that both the L1 and L2 sites are contributing, at 1.8 K, in determining

Table 2: Pigment Composition of Lhca4 and Lhca4-N47H Mutant

	Chl *a*	Chl *b*	Chl/Car	total Car	violax.	lutein	β-Car
Lhca4	7.30	2.70	5.20	1.92	0.16	1.54	0.22
Lhca4-N47H	7.28	2.72	5.50	1.82	0.20	1.49	0.13

the carotenoid triplet populations observed. In fact, the vicinity of *all* the detected carotenoid triplet states to the red chlorophylls, proven by the presence of a bleaching at about 710 nm in the Q_y absorption region of Chls observed in the T-S spectra taken at various frequencies in the whole range of the $2|E|$ transition, points toward the involvement of the carotenoids bound in the site L2, since only these are expected to be close to the red Chls in Lhca4. Thus, a possible assignment of the four components is the following: it is suggested that the site L1 is entirely occupied by lutein as found for several Lhc proteins (*38*), while violaxanthin and beta-carotene only contribute, together with lutein, to the occupancy of the site L2. The ratio 0.16:0.54:0.22, corresponding to violaxanthin, lutein, and β-Car in site L2, would be close to the relative contribution of the three main components in the ODMR spectra. The forth component then, could belong to lutein triplet state in L1 site, where the probability of forming triplet states is expected to be very low and the signal intensity would prevent the detection of the Chl interaction band, which should be found in such a case at wavelengths shorter than 700 nm.

Alternatively, the presence of four distinguishable carotenoid triplet states may be derived from slightly different conformations of pigments and/or protein in the L2 site, rather than from the different carotenoids. This could be the case if the site would be more important in determining the characteristics of the triplet states than the differences in electronic structure of the three carotenoids present in the sample. We favor this second explanation on the basis of the dependence of the signals on the increase of the temperature which leads to a reduction of the number of components needed to describe the line shape of the FDMR transitions. The reduction is likely due to a diminished number of averaged conformations while a selection among different carotenoids with the temperature is not expected. The ZFS parameters at higher temperatures are both reduced (about 10%) compared to the mean values found at low temperature (Table 1). The details of the analysis of the temperature dependence in terms of the different components, as derived by the fitting of the FDMR spectra taken at different temperatures, are available as Supporting Information. Interestingly, ODMR experiments performed in LHC-II showed also the presence of at least three triplet populations at cryogenic temperatures which were difficult to assign only on the basis of the carotenoid composition (*25*, *39*). The T-S spectrum detected at 160 K shows that the T-T absorption maximum, at 527 nm, is close to the low temperature value indicating that the electronic structure of the carotenoid triplet states is only slightly affected by the "conformational changes" reached at higher temperatures.

The carotenoids carrying the triplet states upon illumination at low temperature have a T-T absorption maximum at 525−530 nm and correspondingly a S_2-S_0 bleaching at about 500−510 nm. Compared to the absorption of lutein and violaxanthin in vitro, the absorption of both singlet and triplet states is largely red-shifted, as already observed relative to other Lhc proteins (*20*). Thus, in the Lhca4 complex, the protein environment plays an important role in the tuning of the spectroscopic properties of carotenoids in terms of both polarizability of the surrounding residues and backbone distortions of the molecules.

The dependence on the emission wavelength of the FDMR spectra shows that the four components belong to triplet populations connected via singlet energy transfer, but with different efficiency, to Chls emitting at 690 nm. The incomplete funneling of the energy to red forms in our sample is also confirmed by the presence of Chl triplet states, belonging to the bulk Chls, having an absorption maximum around 675 nm, which are not quenched by carotenoid triplet states. The presence of uncoupled or weakly coupled Chls in *r*-Lhca4 has been previously reported (*24*) and could be due to the monomeric state of the reconstituted complex, as compared to the "in vivo" assembly, where the functional state is represented by a Lhca1−Lhca4 dimer. On the other hand, we cannot exclude that different conformations of Lhc proteins include the presence of proteins lacking the red forms, which could also be compatible with the presence of a residual fluorescence at 690 nm in the 1.8 K emission spectrum, and having a reduced carotenoid−chlorophyll interaction.

In accordance to the CD spectra of Lhca4, the chlorophyll dimer, responsible for the red emission of the complex, has a high-energy exciton band located at about 683 nm (*10*). The recent structure of LHC-I confirms that two chlorophylls (analogous of A5 and B5 in the Kuhlbrandt labeling of LHC-II Chls) are close to each other and may be responsible for the splitting observed in the CD spectrum. We have not observed a bleaching of the 683 nm band accompanying the bleaching at 710 nm in our T-S spectra, indicating either a geometry of the dimer which gives an asymmetric distribution of the dipole strength of the two exciton transitions in the absorption spectrum (however, this possibility seems to in be in contrast with the geometry suggested by the X-ray structure and with the results of the analysis of the absorption spectrum (*10*)) or a canceling net effect in the difference spectrum which precludes a clear evidence of the 683 nm band.

Lhca4-N47H. The effect of the Asn → His substitution on the spectroscopic properties of the reconstituted Lhca4 complex has been previously reported (*10*). In particular, based on the comparison of the LD and CD spectra of Lhca4-N47H with those of the Lhca4, it has been suggested that the Chl A5, which is coordinated by Asn47 in the WT, changes its absorption upon mutation shifting toward the blue, without changing its orientation. No changes in the carotenoid orientation seem to occur. The X-ray structure of plant PSI shows that Chls A5 and B5 of the Lhca1−4 proteins are tilted at different degrees, depending on the Lhca polypeptide, with respect to LHC-II and may be indeed the site of a specific interaction (*5*, *6*, *8*). We have shown that the capability of populating carotenoid triplet states, observed in Lhca4, is conserved also in the Lhca4-N47H mutant. However, significant changes in the spectroscopic properties of both carotenoid and chlorophyll triplet states are found. The efficiency of the Chl triplet quenching by carotenoids is not complete, and unquenched triplet states may be assigned to different populations absorbing at short wavelengths (670 nm), as in the Lhca4 sample, but also at the

Table 3: ZFS Parameters of the Four Components of the Global Fit of FDMR and ADMR Spectra of Carotenoids of Lhca4-N47H Mutant

components (1.8K)	$\|D\|$ (cm^{-1})	$\|E\|$ (cm^{-1})
T_1	362.1×10^{-4}	36.4×10^{-4}
T_2	381.0×10^{-4}	38.0×10^{-4}
T_3	394.5×10^{-4}	39.7×10^{-4}
T_4	397.0×10^{-4}	41.2×10^{-4}
components (160 K)	$\|D\|$ (cm^{-1})	$\|E\|$ (cm^{-1})
T_1	360.1×10^{-4}	36.1×10^{-4}
T_2	378.2×10^{-4}	36.6×10^{-4}

longest ones (690 nm). The mutation thus disturbs the efficiency of the triplet quenching which is optimized for red Chls in Lhca4. In the global fitting procedure for the analysis of the FDMR and ADMR spectra, already described for the Lhca4 protein, the minimum number of components results to be also in this case four and a good fitting may be obtained using roughly the same components as for Lhca4 with different relative amplitudes and little changes of the ZFS parameters (see Table 3 and Supporting Information for details). The effect of the temperature on the carotenoid triplet state signals is also similar to that discussed for Lhca4. At temperature around 150 K, the signal gains again intensity and the number of resolved components is reduced to two (not shown, see Table 3). The conserved number of components, with respect to the WT, may be easily explained if the effect induced by the mutation consists of altering the Chl A5 binding site and the interaction of Chl A5 with the nearby Chls and carotenoid, conserving nevertheless the localization of the triplet state in the L2 site, as in the WT. The redistribution of the relative contribution of the single components as compared to those of Lhca4 could be due to a change in the Chl A5 site leading in turn to a change of the possible arrangements of the carotenoids in site L2. Blue-shifts of few nanometers of the triplet and singlet absorption spectrum of carotenoids are found in the mutant; the main contribution in the T-T absorption region is centered a 525 nm with a shoulder at 505−510 nm associated with the higher frequency components in the microwave spectrum. The change of the optical spectroscopic properties of the carotenoids observed in the mutant, as a consequence of the change in the coordination of the nearby Chls, indicates that the pigments must be considered an optically coupled system.

In the region of Q_y transition bands of chlorophyll interacting with the carotenoids, the main contribution is the bleaching at 688 nm which is, possibly, the uncertainty being due to the low signal-to-noise ratio, accompanied by the presence at shorter wavelengths of a weak bleaching at about 680 nm. We assign this bleaching to the Chl A5 or to some exciton band involving Chl A5 and the nearby chlorophyll molecules in the mutant. The same Chl gives also the detectable triplet state which has an ADMR band at 690 nm because the triplet population is only partially quenched by carotenoids, due to the loss of efficiency in the quenching.

In previous work, the Chl A5 absorption maximum of the Q_y band of the mutant was found at 676 nm (*10*); however, the low-temperature fluorescence spectrum (Figure 1) is inhomogeneously broadened and shows the presence of a band at about 702 nm, indicating that a Chl absorption form is present in the mutant protein absorbing at wavelengths longer than 680 nm. The 702 nm emission band, which is present in the mutant, is very similar to the emission of Lhca2 WT which has indeed a His as ligand for Chl A5. Recently, it has been determined that in Lhca2 the 702 nm emission originates from an absorption band at 690 nm (*40*). Here, the T-S spectra also show the presence of a Chl form at this wavelength, thus suggesting that in the mutant part of the red absorption is shifted indeed to 690 nm. In principle, we cannot exclude that different arrangements of the A5 Chl with respect to B5 in the structure of the mutant lead to Chl populations characterized by different absorption maxima. Only the red-most Chls however give triplet states which are partially quenched by the carotenoid of the L2 site.

CONCLUSIONS

Evidence that carotenoid triplet formation can be induced in the Lhca4 subunit of peripheral light harvesting complex LHC-I has been provided. The highest Chl triplet quenching efficiency has been found in Lhca4 for the red-most Chls suggesting a physiological meaning. Being situated at the bottom of the energy transfer chain, these molecules have the highest probability for intersystem crossing to the triplet states due to the considerably longer lifetime of their singlet excited states. However, Chl−Car distances and interactions in L2 site have been optimized to give a 100% efficiency in the quenching of red-Chl triplet states, even at cryogenic temperature.

Although Chl triplet states have been detected in the sample, it has been demonstrated that they are not localized in the red-most pigments. They are due either to Chls which are weakly connected in the isolated complexes and may belong to "linker" chlorophylls which transfer the excitation to other complexes in the natural environment or to a protein population characterized by a folding lacking the red forms and, for some structural reason, weakly protected by carotenoids.

The N47H mutation introduced disturbs the triplet quenching efficiency of carotenoids in the L2 site. From the comparison of the ODMR results in the WT and in the Lhca4 mutant, we come to the conclusion that the optical properties of the red Chl coordinated by Asp 47 and the Car in the L2 site are both affected by the mutation, meaning that the pigments are coupled to some extent. Spatial coordinates of both Car and Chl molecules are required for a quantitative analysis of the interaction which is, in any case, beyond the scope of the present paper.

In L2 site carotenoids may undergo slightly different conformational arrangements which are reflected in their spectroscopic properties both in the singlet and triplet state. This flexibility is probably related to the capability of the L2 site to accept different carotenoids.

ACKNOWLEDGMENT

We thank Roberta Croce for the helpful discussion and suggestions.

SUPPORTING INFORMATION AVAILABLE

Tables containing the detailed parameters used in the simulation of the FDMR and ADMR spectra of Lhca4 and N47H mutant and a figure showing the results of analysis of FDMR data as a function of temperature. This material

is available free of charge via the Internet at http://pubs.acs.org.

REFERENCES

1. Bassi, R., and Simpson, D. (1987) Chlorophyll-protein complexes of barley Photosystem I, *Eur. J. Biochem. 163*, 221−230.
2. Nilsson, A., Stys, D., Drakenberg, T., Spangfort, M. D., Forsén, S., and Allen, J. F. (1997) Phosphorylation controls the three-dimensional structure of plant light harvesting complex II, *J. Biol. Chem. 272*, 18350−18357.
3. Allen, J. F. (1992) Protein phosphorylation in regulation of photosynthesis, *Biochim. Biophys. Acta 1098*, 275−335.
4. Pichersky, E., and Jansson, S. (1996) in *Oxygenic Photosynthesis: The Light Reactions* (Ort, D. R., and Yocum, C. F., Eds) pp 507−521, Kluwer Academic Publishers, Norwell, MA.
5. Liu, Z. F., Yan, H. C., Wang K. B., Kuang T. Y., Zhang J. P., Gui L. L., An X. M., and Chang, W. R. (2004) Crystal structure of spinach major light-harvesting complex at 2.72 Å resolution, *Nature 428*, 287−292.
6. Kühllbrandt, W., Wang, D. N., and Fujiyoshi, Y. (1994), Atomic model of plant light-harvesting complex by electron crystallography, *Nature 367*, 614−621
7. Caffarri, S., Croce, R., Breton, J., and Bassi, R. (2001) The major antenna complex of Photosystem II has a xanthophyll binding site not involved in light harvesting. *J. Biol. Chem. 276*, 35924−35933.
8. Ben-Shem, A., Frolow, F., and Nelson, N. (2003) Crystal structure of plant Photosystem I, *Nature 426*, 630−635.
9. Schmid, W. H. R., Cammarata, K. V., Bruns B. U., and Schmidt G. W., (1997) In vitro reconstitution of the photosystem I light-harvesting complex LHCI-730: heterodimerization is required for antenna pigment organization, *Proc. Natl. Acad. Sci. U.S.A., 94*, 7667−7672.
10. Morosinotto, T., Breton, J., Bassi, R., and Croce, R., (2003) The nature of a chlorophyll ligand in Lhca proteins determines the far red fluorescence emission typical of photosynthesis, *J. Biol. Chem. 278*, 49223−49229.
11. Schmid, V. H. R., Potthast, S., Wiener, M., Bergauer, V., Paulsen, H. M., and Storf, S. (2002) Pigment binding of photosystem I light-harvesting proteins, *J. Biol. Chem. 277*, 37307−37314.
12. Castelletti, S., Morosinotto, T., Robert, B., Caffarri, S., Bassi, R., and Croce, R., (2003) Recombinant Lhca2 and Lhca3 subunits of the photosystem I antenna system, *Biochemistry 42*, 4226−4234.
13. Croce, R., Morosinotto, T., Castelletti, S., Breton, J., and Bassi, R. (2002) the Lhca antenna complexes of higher plants photosystem I, *Biochim. Biophys. Acta 1556*, 29−40.
14. Formaggio, E., Cinque, G., and Bassi, R. (2001) Functional architecture of the major light-harvesting complex from higher plants, *J. Mol. Biol. 314*, 1157−1166.
15. Cogdell, R. J., and Frank, H. A. (1987) How carotenoids function in photosynthetic bacteria, *Biochim. Biophys. Acta 895*, 63−79.
16. Ruban, A., and Horton, P., (1999) The Xanthophyll cycle modulates the kinetics of non photochemical energy dissipation in isolated light-harvesting complexes, intact chloroplasts, and leaves of spinach, *Plant Physiol. 119*, 531−542.
17. Morosinotto, T., Castelletti, S., Breton, J., Bassi, R., and Croce, R. (2002) Mutation analysis of Lhca1 antenna complex, *J. Biol. Chem. 277*, 36253−36261.
18. Santabarbara, S., and Carbonera, D. (2005), Carotenoid triplet states associated with the long-wavelength-emitting chlorophyll forms of photosystem I in isolated thylakoid membrane, *J. Phys. Chem. 109*, 986−991.
19. Carbonera, D., Giacometti, G., Agostini, G., and Toffoletti, A. (1989) ESP spectra of a carotenoid pigment in LHCII complexes, *Gazz. Chim. Ital. 119*, 225−228.
20. Van der Vos, R., Carbonera, D., and Hoff, A. J. (1991), Microwave and optical spectroscopy of carotenoid triplets in light-harvesting complex LHCII of spinach by absorbance-detected magnetic resonance, *Appl. Magn. Res. 2*, 179−202.
21. Barzda, V., Peterman, E. J. G., van Grondelle, R., and van Amerongen, H., (1998) The influence of aggregation on triplet formation in light-harvesting chlorophyll a/b pigment−protein complex II of green plants, *Biochemistry 37*, 546−551.
22. Peterman E. J. G., Dekker, J., van Grondelle, R., and van Amerongen, H. (1995) Chlorophyll a and carotenoid triplet states in light-harvesting complex II of higher plants, *Biophys. J. 69*, 2670−2678.
23. Lampoura, S. S., Barzda, V., Owen, G. M., Hoff, A. J., and van Amerongen, H. (2002) Aggregation of LHCII leads to a redistribution of the triplets over the central Xanthophylls in LHCII, *Biochemistry 41*, 9139−9144.
24. Melkozernov, A. N., Lin, S., Schmid, V. H. R., Paulsen, H., Schmidt, G. W., and Blankenship, R. E. (2000), Ultrafast excitation dynamics of low energy pigments in reconstituted peripheral light-harvesting complexes of photosystem I, *FEBS Lett. 471*, 89−92.
25. Carbonera, D., Giacometti, G., and Agostini, G. (1992), FDMR of carotenoid and chlorophyll triplets in light-harvesting complex LHCII of spinach, *Appl. Magn. Res. 3*, 859−872, 361−368.
26. Carbonera, D., Giacometti, G., and Agostini, G. (1994) A well resolved triplet minus singlet spectrum of P680 from PSII particles, *FEBS Lett. 343*, 200−204.
27. Carbonera, D., Giacometti, G., Agostini, G., Angerhofer, A., and Aust, V. (1992) ODMR of carotenoid and chlorophyll triplets in CP43 and CP47 complexes of spinach, *Chem. Phys. Lett. 194*, 275−281.
28. Hoff, A. J. (1989) in *Advanced EPR: Applications in Biology and Biochemistry* (Hoff, A. J., Ed.) p 633, Elsevier, Amsterdam.
29. Morosinotto, T., Baronio, R., and Bassi, R. (2002) Dynamics of chromophore binding to Lhc proteins in vivo and in vitro during operation of the xanthophyll cycle, *J. Biol. Chem. 277*, 36913−36920.
30. Gilmore, A. M., and Yamamoto, H. Y. (1991) Zeaxanthin formation and energy-dependent fluorescence quenching in pea chloroplasts under artificially mediated linear and cyclic electron transport, *Plant Physiol. 96*, 635−643.
31. Croce, R., Canino, G., Ros, F., and Bassi, R. (2002) Chromophore organization in the higher-plant photosystem II antenna protein CP26, *Biochemistry 41*, 7343−7343.
32. Hoff, A. J. (1995) Optically Detected Magnetic Resonance (ODMR) of triplet states in photosynthesis, in *Advances in Photosynthesis Vol. 3, Biophysical Techniques in Photosynthesis* (Amesz, J., and Hoff, A. J., Eds.) pp277−298, Kluwer Academic Publisher, New York.
33. Angerhofer, A., Bornhauser, F., Gall, A., and Cogdell, R. J. (1995) Optical and optically detected magnetic resonance investigation on purple photosynthetic bacterial antenna complex, *Chem. Phys. 194*, 259−274.
34. Hala, J., Searle, G. F. W., Schaafsma, T. J., van Hoek, A., Pancoska, P., Blaha, K., and Vacek, K. (1986), Picosecond laser spectroscopy and optically detected magnetic resonance on a model photosynthetic system, *Photochem. Photobiol. 44*, 527−534.
35. Ullrich, J., Speer, R., Greis, J., Von Schütz, J. U., Wolf, H. C., and Cogdell, R. J. (1989) Carotenoid triplet states in pigment−protein complexes from photosynthetic bacteria: absorption-detected magnetic resonance from 4 to 225 K, *Chem. Phys. Lett. 155*, 363−370.
36. Carbonera, D., Giacometti, G., and Agostini, G., (1995) FDMR spectroscopy of peridinin-chlorophyll-a protein from *Amphidinium carterae*, *Spectrochim. Acta, A51*, 115−123.
37. Croce, R, Weiss, S., and Bassi, R. (1999) Carotenoid-binding sites of the major light-harvesting complex II of higher plants, *J. Biol. Chem. 274*, 29613−29623.
38. Morosinotto, T., Caffarri, S., Dall'Osto, L., and Bassi R. (2003) Mechanistic aspects of the xanthophyll dynamics in higher plant thylakoids, *Physiol. Plant. 119*, 347−354.
39. van der Vos, R., Franken, E. M., and Hoff, A. J. (1994) ADMR study of the effect of oligomerisation on the carotenoid triplets ana on triplet−triplet transfer in light harvesting complex II (LHC II) of spinach, *Biochim. Biophys. Acta 1188*, 243−250.
40. Croce, R., Morosinotto, T., Ihalainen, J. A., Chojnicka, A., Breton, J., Dekker, J. P., van Grondelle, R., and Bassi R. (2004) Origin of the 701-nm fluorescence emission of the Lhca2 subunit of higher plant Photosystem I, *J. Biol. Chem. 279*, 48543−48549.

BI050260Z